ORIGINAL PAPER

Optimisation of a PMAxx™-RT-qPCR Assay and the Preceding Extraction Method to Selectively Detect Infectious Murine Norovirus Particles in Mussels

Ravo M. Razafimahefa[1] · Louisa F. Ludwig-Begall[1] · Françoise S. Le Guyader[2] · Frédéric Farnir[3] · Axel Mauroy[4] · Etienne Thiry[1]

Abstract

Human noroviruses are a major cause for gastroenteritis outbreaks. Filter-feeding bivalve molluscs, which accumulate noroviruses in their digestive tissues, are a typical vector for human infection. RT-qPCR, the established method for human norovirus detection in food, does not allow discrimination between infectious and non-infectious viruses and can overestimate potentially infectious viral loads. To develop a more accurate method of infectious norovirus load estimation, we combined intercalating agent propidium monoazide (PMAxx™)-pre-treatment with RT-qPCR assay using in vitro-cultivable murine norovirus. Three primer sets targeting different genome regions and diverse amplicon sizes were used to compare one-step amplification of a short genome fragment to three two-step long-range RT-qPCRs (7 kbp, 3.6 kbp and 2.3 kbp amplicons). Following initial assays performed on untreated infectious, heat-, or ultraviolet-inactivated murine noroviruses in PBS suspension, PMAxx™ RT-qPCRs were implemented to detect murine noroviruses subsequent to their extraction from mussel digestive tissues; virus extraction via anionic polymer-coated magnetic beads was compared with the proteinase K-dependent ISO norm. The long-range RT-qPCR process detecting fragments of more than 2.3 kbp allowed accurate estimation of the infectivity of UV-damaged murine noroviruses. While proteinase K extraction limited later estimation of PMAxx™ pre-treatment effects and was found to be unsuited to the assay, magnetic bead-captured murine noroviruses retained their infectivity. Genome copies of heat-inactivated murine noroviruses differed by 2.3 $\log_{10}$ between RT-qPCR and PMAxx™-RT-qPCR analysis in bivalve molluscs, the PMAxx™ pre-treatment allowing a closer approximation of infectious titres. The combination of bead-based virus extraction and PMAxx™ RT-qPCR thus provides a more accurate model for the estimation of noroviral bivalve mollusc contamination than the conjunction of proteinase K extraction and RT-qPCR and has the potential (once validated utilising infectious human norovirus) to provide an added measure of security to food safety authorities in the hazard assessment of potential bivalve mollusc contamination.

Keyword Norovirus · PMAxx™ · Bivalve molluscs · Diagnosis

Introduction

Human noroviruses (HuNoVs) are the major global cause of non-bacterial gastroenteritis (Koo et al. 2013; Rha et al. 2016; Weinberg 2018), causing approximately 70 000–200 000 deaths annually (Payne et al. 2013). HuNoVs are also the primary cause of viral foodborne gastroenteritis worldwide (Atmar et al. 2018; de Graaf et al. 2016). HuNoVs are frequently detected in environmental waters, contamination being mainly due to improperly treated sewage, floods and waste discharge (Richards, 2001) and typically contaminate raw foods such as fruit (red berries), vegetables (salads) (Cook et al. 2019) and shellfish (molluscs) (Mathijs et al. 2012; Razafimahefa et al. 2019). Filter-feeding bivalve molluscs typically bioaccumulate 100 times more pathogens than their harvesting area (Burkhardt and Calci 2000) and are frequently contaminated with noroviruses since they bind viral particles contaminating the waters they filter (Le Guyader et al. 2006). Even after 48 h of depuration, noroviruses persist in shellfish tissues (stomach, digestive tissues, adductor muscles, haemolymph cells) (McLeod et al. 2017). Bivalve molluscs, which are often eaten raw or only slightly cooked, are consequently often notified as contaminated with HuNoVs through the European Food Alert System for Food and Feed (RASFF). The genus *Norovirus* belongs to the family *Caliciviridae*. According to their polymerase and complete capsid protein sequences, noroviruses comprise 10 genogroups (GI to GX) and 49 genotypes (Chhabra et al. 2019). GI, GII, GIV, and the new GVIII (previous GII.15) and GIX are found primarily in humans (de Graaf et al. 2016). A standardised method to extract HuNoVs from bivalve molluscs consists of an enzymatic method based on proteinase K-assisted extraction (ISO 15,216-1: 2017). Since the proteinase K enzymatic digestion has been shown to have an impact on the infectivity of extracted virus particles (Langlet et al. 2018), other methods have been proposed and are in use to improve the recovery of infectious virus particles. The elution-concentration approach is commonly applied (Polo et al. 2018; Stals et al. 2012). The development of the HuNoV B cell culture system as well as the advent of human organoid cultures have allowed successful in vitro propagation of HuNoV strains (Costantini et al. 2018; Ettayebi et al. 2016; Jones et al. 2014, 2015). However, both approaches are yet too labour-intensive and complex for routine analysis. The use of HuNoV surrogates, such as the closely related murine norovirus (MNV), has thus been found useful to mimic HuNoV behaviour (Cromeans et al. 2014). While molecular techniques for virus detection, such as the ISO 15,216–1 (2017), are highly sensitive, the detection of viral genomes by RT-qPCR is not directly correlated with the presence of potentially infectious virus in a sample. Indeed this approach allows the detection of all virus particles, rendering a true infectious viral hazard assessment impossible. Different treatments and/or environmental conditions (also food or biological variations) may impact the integrity of virus particles; heat mainly affects the viral capsid (denaturation of capsid proteins), UV light and chlorine target the viral capsid and also the genome (Nuanualsuwan and Cliver 2002; Wigginton et al. 2012; Wigginton and Kohn 2012). The establishment of methods that reliably detect only infectious viruses and allow the distinction between infectious and non-infectious particles is needed for accurate hazard assessment of food contamination.

Focusing on both the integrity and the function of the capsid, and also the integrity of the genome provides complete information on the infectivity of virus particles. Detection methods which investigate capsid integrity include enzymatic pre-treatments, e.g. the use of RNase prior to RT-PCR (Li et al. 2012; Nuanualsuwan and Cliver 2002; Topping et al. 2009). In the case of pre-existing capsid damage, the enzyme can enter the virion and disrupt internal nucleic acids, rendering particles with damaged capsids (i.e. non-infectious particles) undetectable by RT-PCR. Recently, intercalating dyes have been used to differentiate potentially infectious particles with intact capsids from non-infectious particles with damaged capsids. The method consists of a pre-treatment with an intercalating dye, such as ethidium monoazide (EMA) or propidium monoazide (PMA), followed by RT-PCR. EMA and PMA are DNA-intercalating dyes with a photo-inducible azide group that covalently cross-links to DNA through visible-light photoactivation. If a viral capsid is intact, EMA or PMA cannot penetrate into virus particles; damaged particles, however, become permeable. Once EMA or PMA has entered the virus particle, the photo-inducible azide group can covalently cross-link the viral genome; in the case of RNA viruses, PMA is postulated to intercalate secondary structures produced by genome folding. The RNA-PMA complex cannot be amplified during the subsequent RT-PCR assay. PMA has been shown to reduce detection of norovirus genome copies by approximately a 1 $\log_{10}$ reduction after five-minute heat treatments of 72 °C (Karim et al. 2015), by a $\log_{10}$ reduction factor of 3.6 after one-minute treatments of 90 °C (Lee et al. 2015), and by a $\log_{10}$ reduction factor of 0.67 after exposure to 65 °C for ten minutes (Leifels et al. 2015). Differences in PMA treatment efficacy and poor repeatability of assays are probably due to the fact that different subsets of primers (differing amplicon lengths and positions on the viral genome) amplify fragments with varying complexities of RNA secondary structures that present differently potent targets to the intercalating agent (Manuel et al. 2018). Recently, the enhanced version of PMA, PMAxx™, has

been demonstrated to have the same spectral properties as PMA and to be more effective than PMA at infectious versus non-infectious discrimination by viability PCR (Randazzo et al. 2016, 2018).

Here, the objective is to determine whether the use of different primer sets in otherwise comparable assays yields varying results as regards the effect of an intercalating pre-treatment and whether PMAxx™ pre-treatment before RT-qPCR analysis can improve the accuracy of the assay in predicting viral infectivity. We compared the detection of short MNV genome fragments in a simple Phosphate Buffered Saline (PBS) matrix by one-step RT-qPCR with long fragment analysis using a poly(T) primer for RT subsequent to PMAxx™ treatment. We further performed a one-step RT-qPCR in conjunction with a primer set targeting a 159-bp-long amplicon. This RT-qPCR process was then implemented to detect MNV extracted from a complex matrix (mussels' digestive tissues (DTs)). An extraction method based on using magnetic beads coated with an anionic polymer was proposed and was compared to the gold standard to recover a higher quantity of infectious particles from the complex matrix (Fig. 1).

Materials and Methods

Cells and Viruses

Cell Culture

RAW 264.7 (ATCC TIB-71) and HeLa cells were grown at 37 °C with 5% of CO_2 in Dulbecco's modified Eagle's medium (DMEM, Invitrogen) supplemented with 10% of heat-inactivated foetal calf serum (FCS) (BioWhittaker), 2% of an association of penicillin (5000 SI units/mL) and streptomycin (5 mg/mL) (Invitrogen) and 1% HEPES buffer (pH 7.6) (Invitrogen).

Viruses

MNV isolate MNV-1 CW1 (Thackray et al. 2007) was propagated in RAW 264.7 cells. Mengovirus (MgV) vMC_0, a mutant strain deleted for the poly(C) tract of its 5′ non-coding region, was propagated in HeLa cells (Martin et al. 1996). The initial MOI used for propagations was 0.05; following a 3-day incubation, flasks were subjected to
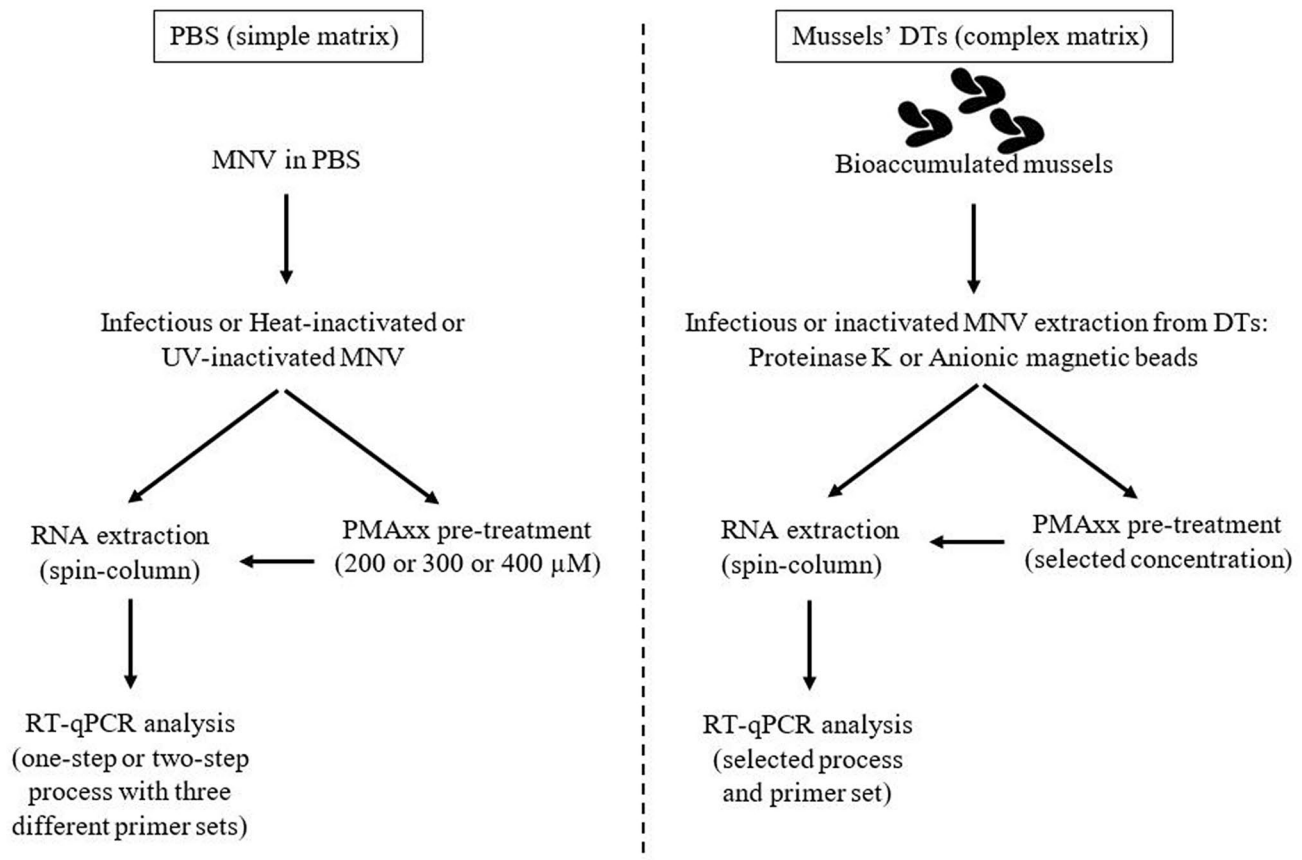

Fig. 1 Flow diagram summarising the objectives of the study

three freeze–thaw cycles. To remove cell debris, cultured MNV and MgV suspensions were centrifuged for 10 min at $4000 \times g$ at 4 °C. The supernatants were transferred to new tubes and were purified over a 5 mL sucrose cushion for 1.5 h at $23,000 \times g$ at 4 °C. The supernatants were then discarded and virus pellets were suspended in PBS and kept at − 80 °C.

Titration of Viruses (TCID$_{50}$ assay)

Infectivity of virus samples was determined via TCID$_{50}$ assay. Briefly, cells were seeded in a 96-well plate at a concentration of 4.10^4 cells per well. Plates were incubated at 37 °C with 5% CO_2 for at least 2 h before infection. Serial tenfold virus dilutions were prepared and added to the wells (50 µL/well). After 2–3 days of incubation, cytopathic effects (CPE) were evaluated under a microscope. Infectious titres were calculated according to the method by Reed and Muench (1938) and were expressed as TCID$_{50}$/mL. Each sample was analysed three times (technical replicates).

Reagents

20 mM propidium monoazide viability dye in H_2O (PMAxx™) was purchased from Biotium (Biotium Inc., Hayward, CA, USA). The surfactant Triton X-100 (Triton) was purchased from Sigma-Aldrich.

Inactivation Treatments

Heat Inactivation

For heat treatment, sealed tubes containing 400–500 µL of virus suspension were immersed in a 90 °C hot water bath for 2 min and were directly cooled on ice.

UV Light Inactivation

For UV treatment, MNV aliquots (400–500 µL) were irradiated for 1 h with an R-52 Grid Lamp (UVP) which emits a uniform 254 nm UV source of high-intensity (200–250 V, 50/60 Hz, 45 AMPS).

Processing of Mussels

Bioaccumulation

Fresh mussels (*Mytilus edulis*) were purchased at a local fish shop. Once arrived in the laboratory, mussels were directly immersed in a tank containing 4–5 L of natural sea water with continuous aeration using a bubble stone fixed to an air pump (Shega Prima). The room temperature was kept at 18 °C. Dead mussels were discarded; mussels were considered dead if they floated in the tank, if they did not open within minutes after immersion in sea water, or if they did not close their valve as a response to manual pressure when outside the water. Mussels were kept for 24 h in their new environment before addition of a suspension of infectious or UV-inactivated MNV at a final concentration of ∼ 10^7 TCID$_{50}$/mL or zero TCID$_{50}$/mL, respectively, of seawater. Ten mL of live phytoplankton (*Nannochloropsis*; Colombo, Netherlands) was added simultaneously to stimulate the bioaccumulation process.

Dissection

Mussels dissected before bioaccumulation were used as negative controls; the remaining mussels were dissected after 24 h of bioaccumulation. The adductor muscle was first cut to open the mussels, and then digestive tissues (DTs) were removed, finely chopped, aliquoted (1 g/tube) and stored at -80 °C before virus extraction.

Optimisation of Virus Extraction

A bead-based virus extraction approach was compared to the proteinase K-dependent method described in ISO standard 15,216–2. Virus extraction experiments were performed in triplicate. MgV was used to validate extraction method efficiency. MgV CM$_0$ (10^7 TCID$_{50}$/mL) were seeded per aliquot of mussel DT before extraction with proteinase K. The latter approach consisted of incubating the mixture of DT and proteinase K (100 µg/mL) for 60 min at 37 °C, followed by 15 min at 60 °C. The mixture was then centrifuged for 15 min at $3000 \times g$.

The magnetic bead assay was developed using 300-nm-diameter viro-adembeads coated with an anionic polymer (polymethyl vinyl ether-maleic anhydride) (Ademtech, Pessac, France). The DTs were homogenised in 1 mL of PBS using a TissueLyser system; DTs were shaken together for 2 min with a 5 mm stainless steel bead at 30 Hz (QIAGEN), and homogenates were subsequently centrifuged (5 min at $3000 \times g$). Simultaneously, 50 µL of viro-adembeads was washed twice with binding buffer and once with PBS. The supernatant was then incubated with 50 µL of washed viro-adembeads for 20 min at room temperature (RT) with slow rotation. The virus-bead conjugates were washed once with 200 µL PBS and resuspended in 750 µL PBS.

PMAxx treatment Prior to RT-qPCR

Initially, three concentrations of PMAxx™, 200, 300 and 400 µM, were tested. PMAxx™ was added at a selected final concentration into each virus suspension, followed by 15 min of incubation in a dark room and activation using a

PhAST blue Photo-Activation System for Tubes (GenIUL) for 15 min.

Triton was added to PMAxx™ at 0.5% to enhance the entry of PMAxx into virus particles with only partially compromised capsids. The performances of PMAxx™ and PMAxx™-triton were compared. Reduction of genome copies obtained after PMAxx™ (-triton) treatment was compared with untreated-PMAxx™ samples. Infectivity and genome copies were determined as described above.

Detection Limit of the Magnetic Beads Assay

The determination of the detection limit of the magnetic beads assay was performed using tenfold serial dilutions of the homogenates obtained after homogenisation and centrifugation in PBS prior to the magnetic beads capture and followed by RNA extraction and RT-qPCR analysis as described below.

Optimisation of PCR Conditions

Viral RNA extraction

RNA was extracted from 140 µL purified viral suspension using the QIAamp Viral RNA Mini Kit (Qiagen, Valencia, CA, USA) following manufacturer's instructions. The nucleic acid was eluted in 60 µL elution buffer and stored at -20 °C for subsequent analysis.

Quantitative RT-PCR and Rationale for Primer Design

Of the three primer sets used for comparison, two primer sets were selected from MNV PMA studies in the literature according to their target region localisation, size and minimum free energy (Supplementary Table 1). Both 159 and 70 primer sets target the open reading frame 1 (ORF1) (localisations: 3727–3885 and 5036–5105 nucleotides, respectively). The third R1 primer set, previously implemented by Mathijs et al. (2010), targets the ORF1 to the 5′ genome end (389–472). According to RNAfold secondary structure predictions (http://rna.tbi.univie.ac.at/cgi-bin/RNAWebSuite/RNAfold.cgi), the minimum free energy of the three targeted regions is between -38.09 and -21.80 kcal/mol. Since the primer sets target three different regions, the RT-qPCR with a long-range RT allows the detection of different product sizes.

The RT-qPCR was performed using a CFX96 Touch™ Real-Time PCR Detection System (Bio-Rad) with TaqMan probes. For two-step reactions, cDNA was generated using a poly-A primer starting at the 3′end of the genome using the Superscript III (Invitrogen) kit with 7.5 µL of RNA and 12.5 µL of reaction mix. The qPCR was then performed with 3 µL of cDNA and 7 µL of reaction mix containing the iScript Supermix (Bio-Rad) and 0.2 µM of each primers and probe. The RT-qPCR one-step reaction was performed with an iTaq™ Universal Probes One-Step Kit (Bio-Rad) in a 10 µL reaction volume containing 3 µL of RNA template, 0.2 µM each of forward and reverse primer and 0.2 µM of probe (Supplementary Table 1). Each sample was amplified in triplicate.

Genomic detection of MgV MC_0 for extraction efficiency was carried out with an iTaq™ Universal Probes One-Step Kit (Bio-Rad) (Supplementary Table 1). The Ct value of each samples was compared with the Ct value of the positive control used during the extraction experiment. The efficiency was calculated using the formula $E = 10^{\left(\frac{\Delta Ct}{slope}\right)}$, where E is the efficiency, with an acceptable limit of 1% (ISO 15216_1, 2017).

The cycling conditions for the one-step reaction were as follows: 55 °C for 10 min, 95 °C for 1 min, and 35 cycles of 95 °C for 10 s and 60 °C for 40 s. Two-step cycling was performed as follows: RT 1st step: 65 °C for 5 min; RT 2nd step: 55 °C for 1 h and 70 °C for 15 min and PCR: 95 °C for 5 min and 40 cycles of 95 °C for 15 s and 60 °C for 40 s.

The standard curves for the molecular detection of MNV with different primer sets were performed using MNV RNA of known concentration (Quant-iT™ RiboGreen™ RNA Assay Kit; Molecular Probes, Inc., Invitrogen). All standard curve assays were performed using the Bio-Rad CFX96 Touch™ Real-Time PCR Instrument.

PCR inhibitors, which might either underestimate or prevent detection of viruses, were detected by amplifying the external control (EC or in vitro transcribed RNA). Partial MNV ORF1 (nucleotides 3727 to 3885) was cloned into a pGMT easy vector (Promega). Following vector transformation into and recovery from *Escherichia coli* DH5α competent cells, in vitro transcription of linearised plasmid samples was performed using the HiScribe T7 Quick High Yield RNA Synthesis Kit (BioLabs). After DNase treatment, RNA was purified and quantified using the Quant-iT™ RiboGreen™ RNA Assay Kit (Invitrogen).

An equal volume of EC of 10^5 copies and sample were mixed and amplified in a one-step reaction. The difference of Ct was obtained by subtracting the Ct value of sample mixed with EC to Ct value of EC. The inhibition was calculated using the formula $I = 1 - 10^{\left(\frac{\Delta Ct}{slope}\right)}$ where I is the inhibition; an inhibition superior to 75% was not accepted.

Data Analysis

Means and standard deviations were calculated for each sample group, and were represented graphically using GraphPad Prism 8.4.3 software. The number of genomic copies was analysed using a two-way ANOVA for repeated measurements (after normalisation of the data using a $\log_{10}$ transformation), the two factors being PMAxx™ treatment

or extraction method and RT-qPCR process. P-values < 0.05 were considered significant.

Results

Optimisation of PMAxx-RT-qPCR Assay for the Selective Detection of Infectious MNV in PBS

Standard curves were performed using three primer sets. The detection limits (LoD) of the respective assays were 196 copies/mL for R1 primers, 208 copies/mL for 159 primers, and 112 copies/mL for 70 primers (Supplementary Fig. S1).

The performance of different concentrations of PMAxx™ (200, 300 and 400 µM), a viability PCR dye known to be more efficient than PMA, was compared on PBS suspension samples of untreated MNV, MNV inactivated with temperatures of 90 °C for 2 min, and MNV inactivated via 1 h exposition to UV light. A subsequent RT-qPCR analysis was performed with the three different primer sets to compare a one-step RT-qPCR to a two-step RT-qPCR with long-range RT. The efficiency of PMAxx™ intercalation was demonstrated with naked MNV RNA, extracted from whole virus suspension (Fig. 2A).

For non-inactivated MNV, the genomic copy values obtained via the two-step approach with primer R1 of infectious MNV without PMAxx™ were the most similar to the
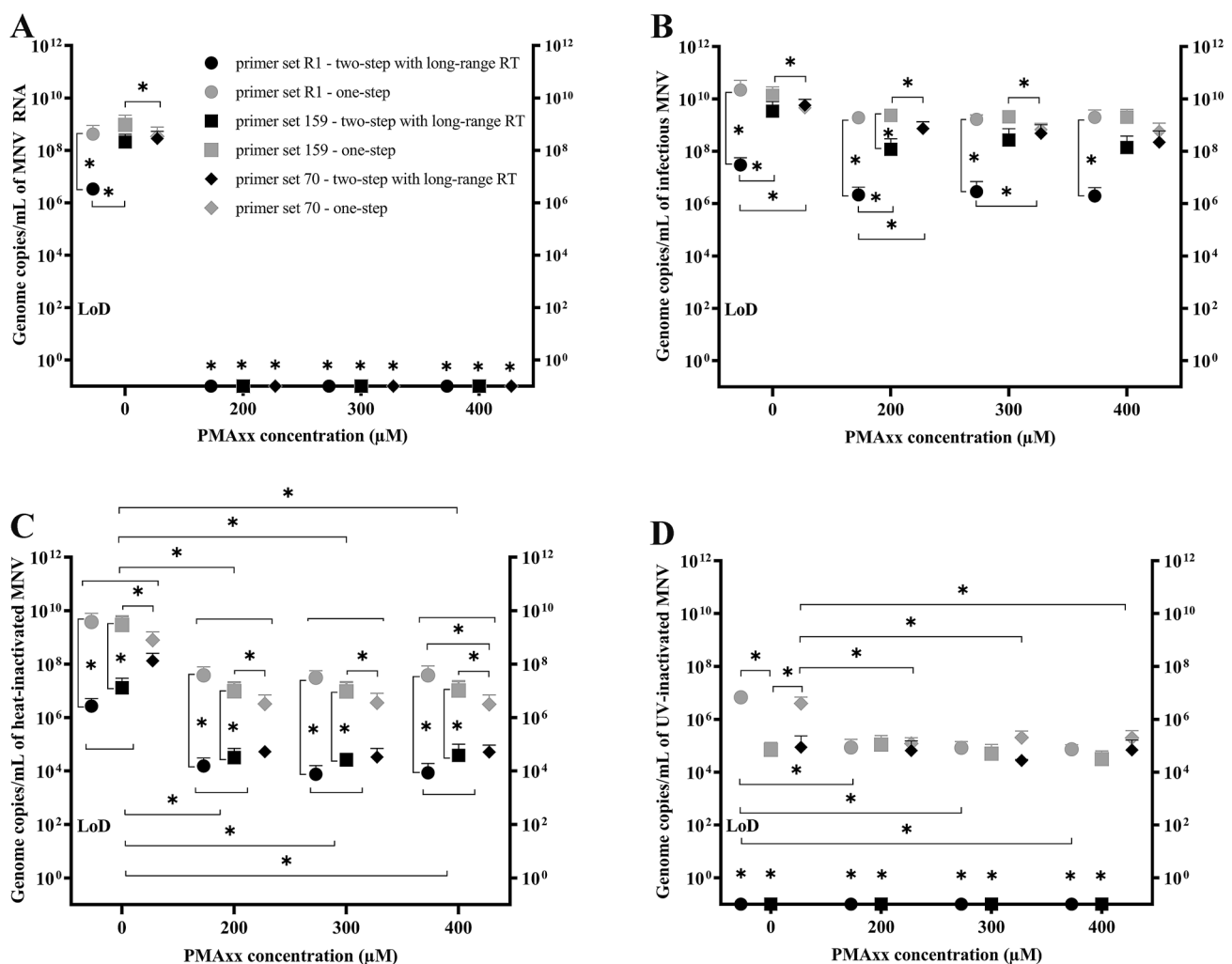

Fig. 2 Comparison between different concentrations (200, 300 and 400 µM) of PMAxx treatment on MNV in PBS and subsequent genome copy number quantification (gc/mL) with two processes: RT-qPCR with long-range RT and one-step RT-qPCR with three different pairs of primers; MNV RNA as positive control **a**, infectious MNV **b**, heat-inactivated MNV **c** and UV-inactivated **d**. The symbols represent the log genome copies of samples with standard deviation bars:

○, primer R1; □, primer 159; ◇, primer 70. LoD: 196 copies/mL for R1 primers, 208 copies/mL for 159 primers, and 112 copies/mL for 70 primers. After inactivation of MNV to heat (90 °C, 2 min) or UV light (1 h), all infectious MNV particles were inactivated. Initial titre of MNV was 8.13×10^6 TCID$_{50}$/mL. Experiments were made in triplicate. *significant differences between means ($p < 0.05$)

infectious titre of 10^7 TCID$_{50}$/mL (Fig. 2B). With the two-step RT-qPCR with long-range RT, genome copy numbers declined gradually the further the primer set was localised from the 3′ genome end; this difference was significant for PMAxx™-untreated samples and those treated with PMAxx™ at 200 µM and 300 µM (Fig. 2B). Contrary to the two-step RT-qPCR assay, genome copy values were constant in the one-step RT-qPCR assay performed with R1 and 159 primers; a log_{10} reduction factor of 0.5 was observed with primer set 70 as compared to primer set 159 (Fig. 2B). The difference between the one-step assay and the long-range-RT-linked two-step approach was greater the further the primers were located upstream of the 5′ end. This was significant for all assays, with a log_{10} reduction factor of 2.7 to 3 for the R1 primer set (Fig. 2B).

Genome copies of heat-inactivated MNV remained detectable by both RT-qPCR approaches. While heat inactivation had no significant effect on genome detection via one-step RT-qPCR, it significantly influenced detection in two-step RT-qPCR assays (Fig. 2B & 2C). Genome copy numbers as quantified by one-step approach with primer sets R1 and 159 were significantly higher compared with the two-step approach for almost all assays; genome copy numbers decreased when the primer set close to the 3′ end. In contrast, for the RT-qPCR with long-range RT approach, genome copy numbers progressed inversely (Fig. 2C). However, no significant difference was observed between the three primer sets in the one-step approach or in the two-step approach for all assays, except for a log_{10} reduction factor of 0.5 of primer set 70 in comparison with primer set 159 in the one-step process. Genomic copy numbers decreased significantly in conjunction with PMAxx™ treatment for all PMAxx™ concentrations in all RT-qPCR processes (2–2.5 log_{10} reduction with one-step process and 2.5 to 3.5 log_{10} reduction with two-step process) (Fig. 2C).

UV-inactivated MNV genomes were not detectable by long-range RT-linked qPCR using primers R1 and 159, which allowed the reverse transcription of 7 kbp and 3.6 kbp of RNA, respectively, with or without PMAxx™ treatment (Fig. 2D). PCR-positive signals were obtained with all three primers in the one-step process and with primer set 70 in the two-step process; a significant reduction of genome copies ($\geq 3 \log_{10}$) was observed compared with non-inactivated MNV (Fig. 2D). The difference between R1 and 159 and also between 159 and 70 primers utilised in the one-step process without PMAxx™ was significant. After PMAxx™ treatment, the same level of genome copies was observed for all PMAxx™ concentrations with the one-step RT-qPCR using the three primer pairs and the two-step RT-qPCR with primer set 70. However, reductions of genome copy values after PMAxx™ treatment in conjunction with the one-step process and primer sets R1 and 70 were significant (Fig. 2D).

In summation, variations in PMAxx™ concentration had no significant effect on detection of MNV in PBS suspension. Genome quantification of non-inactivated and heat-inactivated MNV differed between one-step and two-step processes. While PMAxx pre-treatment did not completely remove RT-qPCR signals of heat-inactivated MNV in either the one-step or two-step assay (absence of infectious particles was confirmed via TCID$_{50}$), the decrease in genome copies was higher for the two-step process. The long-range RT-qPCR capable of detecting fragments of more than 2.3 kbp allowed accurate estimation of infectivity of UV-damaged MNV. Although PMAxx™ pre-treatment affects detection of UV-inactivated MNV when quantified with one-step RT-qPCR process using R1 and 70 primer sets, this is not the case for primer set 159.

Performance of Beads Assay for the Recovery of MNV in PBS

The efficiency of the magnetic bead-based recovery was first tested in a preliminary assay on infectious MNV in PBS. The three test conditions allowed detection of infectious MNV in PBS without significant difference of genome copy values (Supplementary Fig. S2). Subsequent experiments on infectious and inactivated MNV in PBS demonstrated that the anionic beads captured either infectious or heat- and UV-inactivated MNV in PBS (Supplementary Fig. S3).

Performance of Beads Assay for the Recovery of MNV Bioaccumulated in Mussel DTs Compared with Proteinase K Approach

After the performance of anionic beads was demonstrated in PBS, this method was compared with the proteinase K approach for MNV extraction from mussel DTs. It was tested in conjunction with two RT-qPCR approaches and three different primer sets. All samples extracted following the proteinase K method showed valid extraction efficiencies between 2 and 10%. Prior to virus capture, a homogenisation step based on grinding in a bead beating system was performed. The homogenisation step did not cause any detriment to virus infectivity, as tested on MNV in PBS (data not shown). Genome copies quantified subsequent to proteinase K extraction via one-step RT-qPCR with primer sets 159 and 70 were significantly higher (1.2 log_{10}) than those measured subsequent to bead-based extraction. However, contrary to proteinase K extraction, the bead-based assay allowed detection of infectious particles (Fig. 3). Genome copies could be quantified by two-step process with primer set 70 in all assays. Unexpectedly, detection with primer sets 159 and 70 via two-step process with long-range RT was not effective (Fig. 3). The difference between the one-step and two-step processes was significant for almost all assays (Fig. 3).
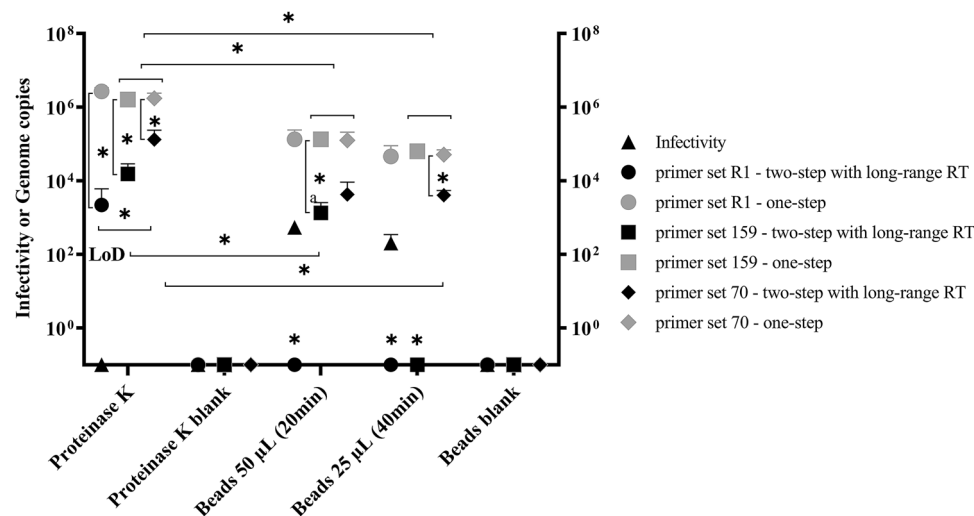
Fig. 3 Comparison between proteinase K and magnetic beads assay for recovering of MNV bioaccumulated in mussels' DTs and subsequent infectivity assay and genomic copy number quantification with two processes: RT-qPCR with long-range RT and one-step RT-qPCR with three different pairs of primers. The symbols represent the infectivity ▲ and the log genome copies (gc/g DTs) of samples with standard deviation bars: ○, primer R1; □, primer 159; ◇, primer 70.

LoD: 196 copies/mL for R1 primers, 208 copies/mL for 159 primers, and 112 copies/mL for 70 primers. MNV titre (10 mL/tank) used for inoculation was 1.9×10^7 TCID$_{50}$/mL. Blank or negative controls correspond to mussel DTs before bioaccumulation. Symbols on the horizontal axis correspond to mean values inferior to limit of detection. Experiments were made in triplicate. [a]Two positive replicates out of threes. *significant differences between means ($p < 0.05$)

Regarding the two conditions of the beads assay (50 μL beads – 20 min and 25 μL – 40 min), there was no significant difference between two different assays. According to these results, the beads assay condition of 50 μL and incubation of 20 min at RT followed by a one-step RT-qPCR process with the 159 primer set (which per its design yields the longest amplicon) were applied to detection of MNV extracted from mussel DTs. The one-step RT-qPCR process with primer set 159 was implemented to determine the detection limit of the magnetic beads assay. The assay was performed on homogenates of bioaccumulated virus to simulate the binding of virus particles to DT tissues. Tenfold serial dilutions realised in PBS showed the lowest detectable concentration of virus captured by the beads to be 300 genome copies per gram (gc/g) DTs. The first dilutions in the series showed the beads to be saturated, this most probably by impurities from the homogenates (Supplementary Fig. S4).

In summary, more efficient extraction of intact infective MNV was achieved implementing the novel bead-based assay than the proteinase K-based ISO norm protocols. The bead-based virus extraction and subsequent one-step RT-qPCR with primer set 159 were applied to test the efficacy of PMAxx to selectively detect infectious MNV.

Efficacy of PMAxx-RT-qPCR Assay for the Selective Detection of Infectious MNV Bioaccumulated in Mussel DTs

The first step for the detection of MNV bioaccumulated in mussel DTs was the bioaccumulation. Infectious and UV-inactivated MNV were inoculated in seawater during bioaccumulation experiments, and then heat inactivation was performed on supernatants of mussel DTs during extraction. Treatments with PMAxx™ (300 μM) and PMAxx™ (300 μM) combined with 0.5% Triton were performed. Results for non-inactivated MNV showed that PMAxx™ assays did not significantly affect the signal for both extraction methods (Fig. 4A). Either PMAxx™ or PMAxx™ combined with Triton did not allow a signal reduction of heat- and UV-inactivated MNV after proteinase K extraction (Fig. 4B & 4C). However, a pre-treatment with PMAxx™ or PMAxx™ combined with Triton significantly reduced (2.3 log$_{10}$) the signal of heat-inactivated MNV after magnetic beads assay (Fig. 4B). No difference in signals was observed between PMAxx™ alone or PMAxx™ combined with Triton for heat-inactivated MNV (Fig. 4B). All signals observed for UV-inactivated MNV
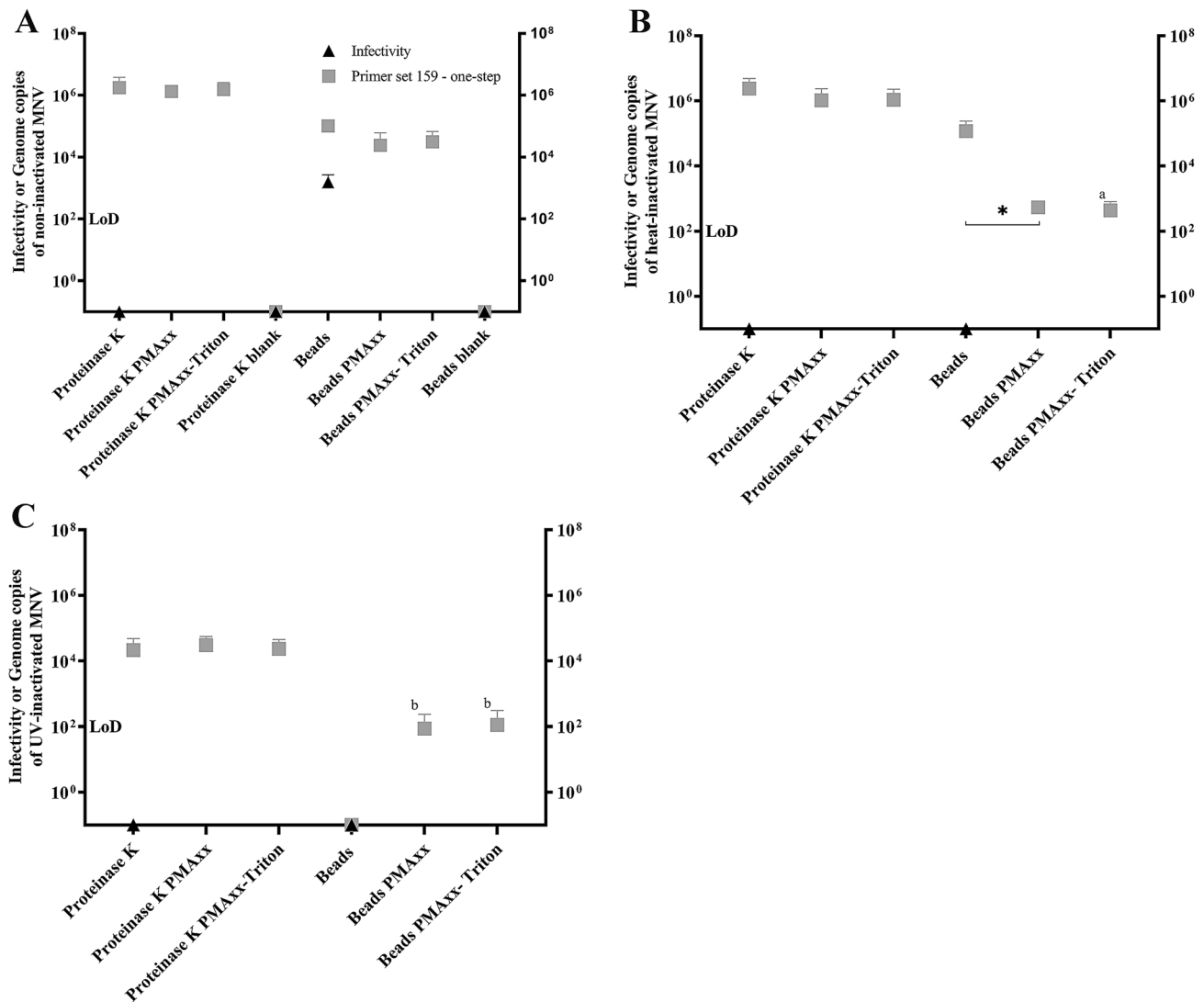
Fig. 4 Comparison between proteinase K and magnetic beads assay for recovering of MNV bioaccumulated in mussels' DT, infectious MNV (**a**), heat-inactivated MNV (**b**) and UV-inactivated (**c**), and subsequent infectivity assay and PMAxx™ (300 μM) or PMAxx™-triton treatment followed by genomic copy number quantification with one-step RT-qPCR. The symbols represent the infectivity ▲ and the log genome copies (gc/g DTs) of samples with standard deviation bars: □, LoD: 208 copies/mL for 159 primers. MNV titre (10 mL/tank) used for inoculation was 1.9×10^7 $TCID_{50}$/mL. Blank or negative controls correspond to mussel DTs before bioaccumulation. Symbols on the horizontal axis correspond to mean values inferior to limit of detection. Experiments were made in triplicate. [a]Two positive replicates out of three. [b]One positive replicate out of three. *Significant differences between means ($p < 0.05$)

extracted by magnetic beads assay were very close to the limit of detection (Fig. 4C).

In conclusion, bead-based MNV extraction prior to PMAxx™-RT-qPCR analysis permitted a 2.3 $\log_{10}$ genome reduction of heat-inactivated MNV; no such reduction was observed with proteinase K extraction.

Discussion

The assessment of public health risks with regard to the detection of norovirus particles from food is hampered both by the lack of a method allowing either the detection

of exclusively intact virus particles and/or the discrimination between infectious and non-infectious viruses, as well as the lack of a standardised method permitting the extraction of intact virus particles from food matrices (a prerequisite to subsequent determination of infectivity).

Here we determine improved experimental conditions for a molecular method permitting an as accurate as possible distinction between infectious and non-infectious (inactivated) norovirus particles and, in a second step, present a novel assay for the extraction of infectious noroviruses from bivalve mollusc matrices, using MNV as an infectious HuNoV surrogate.

Pre-treatments with intercalating agents PMA/PMAxx™, tested in conjunction with different PCR kits, different primer sets, and varying concentrations of intercalating dye, have previously rendered significantly deviant estimations of norovirus genome copy numbers (Karim et al. 2015; Lee et al. 2015; Leifels et al. 2015; Randazzo et al. 2018). To investigate the impact of the different assay conditions and to develop a standardised method of norovirus genome copy estimation, we tested three different primer sets (selected from pertinent literature) in conjunction with two RT-qPCR processes (one-step versus two-step with long-range RT), and three PMAxx™ concentrations to detect MNV in PBS. To model capsid and genome damage (which may occur during treatment at various stages of the food chain) and their respective effect on detection efficacy, capsid-damaging heat- and genome-damaging UV treatments were applied to MNV samples prior to the various RT-qPCR assays.

In a one-step RT-qPCR assay, a PMAxx™-RT-qPCR, i.e. a RT-qPCR involving PMAxx™ pre-treatment, permitted a closer approximation of genome copy numbers and true infectious virus MNV titres than a simple RT-qPCR; heat-treated and untreated MNV copy numbers were identical without PMAxx™ pre-treatment, and heat-treated MNV copy numbers showed a $\log_{10}$ reduction factor of 2 to 3.5 compared with those of untreated MNV with PMAxx™ pre-treatment. While the PMAxx™-RT-qPCR assays were not completely able to distinguish infectious from non-infectious particles (TCID$_{50}$ assays showed heat treatment to have completely inactivated MNV suspended in PBS), the PMAxx™ pre-treatment thus presented a significant improvement to a simple RT-qPCR assay by eliminating 2 to 3.5 $\log_{10}$ MNV particles with damaged capsids from the equation and rendering them undetectable by RT-qPCR. Varying concentrations of PMAxx™ had no significant effect on genome copy numbers, a concentration of 200 µM being sufficient for the pre-treatment of MNV prior to RT-qPCR. However, the RT-qPCR process following PMAxx™ can influence genome reduction. Differing genome copy reductions reported in the current literature are consequently probably not attributable to fluctuations in intercalating dye concentrations (a range of PMA concentrations of 100–348 µM has previously been

tested Karim et al. 2015; Kim and Ko 2012; Lee et al. 2015; Leifels et al. 2015), but are due to the use of differing primer sets and RT-qPCR assay conditions.

In contrast to heat treatment, which acts upon the viral capsid, UV inactivation typically affects the virus genome more strongly. Consequently, it is unsurprising that viral genome copy numbers of UV-treated viruses are typically not affected by PMA treatment; UV-treated viruses, while remaining impermeable to PMA, are nevertheless rendered non-infectious (Karim et al. 2015; Leifels et al. 2015). No genome copies were detected post UV treatment when the assay was performed with primer pairs R1 (7kbp) and 159 (3.6kbp), in which the RT step served to reverse transcribe a cDNA fragment of 7kbp and 3.6kbp, respectively. However, when primer set 70 (2.3 kb cDNA) was implemented, 10^4 genome copies were detected as quantified via one-step RT-qPCR with primer set 159. The one-step approach with primer sets R1 and 70 led to the detection of ~ 10^6 genome copies of UV-inactivated MNV; meanwhile MNV was rendered non-infectious (as measured by TCID$_{50}$ assay). The differences in detection of UV-damaged RNA became more pronounced with the increase of fragment size during the two-step process; this is in line with Li et al. (2014) and Wolf et al. (2009). To distinguish between non-infectious and potentially infectious virus particles, a RT-qPCR assay can thus not rely on interacting pre-treatments but must inherently allow for such a distinction; longer fragment size, permitting a better estimation of genome integrity may be utilised towards this end. Here, we showed that the primer pair 159, targeting a 159 bp long genome fragment, was able to more accurately predict RNA degradation than either primer pair 70 (amplicon length: 70 bp) or R1 (amplicon length: 84 bp) without PMAxx™ pre-treatment in one-step RT-qPCR. We attribute this to the fact that amplification between forward and reverse 159 primers (covering more genome at approximately double the amplicon length of the other primer sets) was more likely to be interrupted at UV-mediated genome breakages. Surprisingly, the observed differences were not conserved in combination with PMAxx™ treatment; the genome copy overestimation of primer pairs 70 and R1 was levelled out subsequent to PMAxx™ treatment and found to be at the same level as 159 primer set genome copy values. We suggest that this effect may be due to the fact that UV-treated viruses were, in fact, not only damaged at the level of their genome (genome damage was not picked up on using small amplicon sizes in a RT-qPCR), but were also compromised at the level of their capsids. PMAxx™ pre-treatment, additionally investigating capsid integrity, thus permitted an estimation of MNV copy numbers that more closely corresponded to true infectivity values.

To allow for an estimation of viral infectivity of viruses transmitted via food matrices, extraction of these viruses

from their vector must proceed in a way that does not damage the virus before it can be analysed. Proteinase K extraction, the current ISO norm for the extraction of noroviruses from food (ISO 15,216-1: 2017), is known to impact the infectivity of extracted viruses (Langlet et al. 2018). Here, we confirm that bioaccumulated MNV extracted from mussel DTs via proteinase K extraction is indeed inactivated by the extraction procedure itself. To address this issue, a novel assay for the extraction of infectious MNV from bivalve mollusc matrices was developed; this method, based on magnetic beads coated with anionic polymer, permits extraction of intact virus particles, representing a significant advantage over current proteinase K-based extraction methods, which damage viral capsids, thus precluding downstream assays to determine viral infectivity. Anionic polymer-coated beads have previously been demonstrated to capture different enveloped and non-enveloped from a range of matrices, including cell culture media, PBS, water, oyster homogenate and seawater (Hatano et al. 2010; Patramool et al. 2013; Sakudo and Onodera 2012; Toldrà et al. 2018). Here, we demonstrate the capacity of anionic beads to capture infectious or inactivated MNV in PBS and from mussel DTs. While fewer genome copies were detected following magnetic bead-based extraction than proteinase K extraction (1.2 $\log_{10}$), the infectivity of captured viruses was retained, a prerequisite for the assessment of public health risks due to infectious virus burdens. The detection limit of the assay was determined to lie around 300 gc/g DTs, coinciding with virus quantities typically contained in shellfish samples (10^2–10^4 gc/g DTs (Stals et al. 2012). To the best of our knowledge, this is the first report using anionic magnetic beads to extract noroviruses from bivalve mollusc DTs, using MNV as an infectious HuNoV surrogate. Polymer-coated magnetic beads are negatively charged, rendering them, in theory, ineligible for the binding of negatively charged MNV particles with an isoelectric point between 3 and 4 (Brié et al. 2017). While other parameters must be involved in the successful interaction with MNV, these are as yet unknown. Similar genome copy values were obtained with all the three primer sets in conjunction with in the one-step process following both proteinase K- and bead-based virus extraction; no genome copies were detected with primer sets R1 and 159 in the long-range RT and qPCR following magnetic bead-based virus extraction. Overall, we judge a one-step PMAxx™ RT-qPCR utilising primer set 159 to amplify a large genome section to be the assay most suitable to provide an improved estimation of genome copy numbers corresponding to potentially infectious virus loads. While a further augmentation of amplicon sizes might increase assay precision and permit a closer approximation of true infectious virus titres, this is limited by restrictions inherent to RT-qPCR protocols. A more pronounced RT-qPCR signal decrease, as achievable in a two-step process, may make for a more closer approximation of infectious titres; however, two-step RT-qPCRs are typically time-consuming and may increase the risk of contamination during a routine analysis. These observations may serve as a benchmark for the development of similar assays for HuNoV detection; we propose that magnetic bead-based virus extraction should be succeeded by a one-step PMAxx™ RT-qPCR amplifying an as large as possible (within the confines of qPCR design) amplicon.

Since infectivity of extracted viruses was retained via magnetic bead extraction, the distinction of infectious and non-infectious virus particles was investigated with PMAxx™ pre-treatment in downstream assays. To account for possible difficulties associated with a more complex matrix, PMAxx™ treatments post MNV extraction were supplemented by the addition of surfactant Titron X-100, as previously described for rotavirus and hepatitis A virus analyses (Coudray-Meunier et al. 2013; Moreno et al. 2015). To further account for increased sample complexity and density (likely presence of debris remaining in virus suspension and possibility of interference with PMAxx™ intercalation), the PMAxx™ concentration was augmented to 300 μM.

Discrimination between untreated or heat-inactivated MNV extracted from bioaccumulated mussels was not possible either via PMAxx™ or PMAxx™-triton RT-qPCR after proteinase K extraction; however, genome copies were detected at high levels in simple RT-qPCR and PMAxx™ or PMAxx™-triton qPCR assays (10^6 gc/g DTs), this in line with Randazzo et al. (2018). In contrast, the bead-based extraction method and subsequent PMAxx™ or PMAxx™-triton RT-qPCR indicated heat-treatment effects by a loss of 2.3 $\log_{10}$ genome copies of heat-treated MNV in comparison to untreated samples. Thus, ~ 10^5 gc/g DTs were detected both in untreated and heat-treated samples in a simple RT-qPCR; meanwhile ~ 10^4 and ~ 10^3 gc/g DTs were detected in untreated and heat-treated sample, respectively, in a PMAxx™ RT-qPCR. Addition of PMAxx™ or PMAxx™-triton did not make a difference to the detection of UV-inactivated non-infectious MNV following proteinase K extraction, further suggesting that viral capsids are no so significantly affected by proteinase K as to render viruses permeable to PMAxx™ post extraction. We attribute the loss of viral infectivity observed post proteinase K extraction to a change in capsid surface conformation (e.g. attachment factors, receptors) rather than complete capsid damage in terms of permeability. The advantage of bead-based method may thus not be only attributable to the fact that it is not a damaging approach, but rather a more stringently purifying one, removing traces of cellular debris from later RT-qPCR reactions. This is supported by recent studies by (Sarmento et al. 2020) which demonstrated that proteinase K HuNoV extraction from naturally contaminated bivalve

molluscs, followed by PMAxx™ treatment, and then magnetic bead RNA extraction, allowed discrimination of infectious and non-infectious HuNoV particles via RT-qPCR (genome copy numbers reduced by up to 3 $\log_{10}$ in a PMAxx™ qPCR assay as opposed to a simple qPCR). The present study utilises the murine norovirus model, which, albeit long considered suitable surrogate to model human norovirus tenacity (Cannon et al. 2006; Cromeans et al. 2014), remains a model and as such may present inherent fallacies. The true ability of the bead-based extraction method combined with PMAxx™-RT-qPCR to distinguish infectious and non-infectious human noroviruses is yet unknown and remains to be tested against potentially infectious human noroviruses particles in conjunction with a system able to measure their infectivity or lack thereof.

Conclusion

In conclusion, the detection of viral genomes via one-step or two-step RT-qPCR with long-range RT processes may highly differ depending on sample treatment. We show that assays aiming at detection of the entire genome allow a better assessment of RNA integrity post UV treatment. We describe the development of an improved one-step PMAxx™ RT-qPCR for discrimination between heat-treated, UV-treated and untreated viruses. Furthermore, we demonstrate a novel magnetic bead-based method for MNV extraction from bivalve mollusc matrices, permitting better downstream discrimination between heat-treated and untreated viruses. This extraction method, combined with the described PMAxx™ RT-qPCR assay, has the potential to be a valuable tool for future detection of infectious noroviruses, permitting more accurate assessment of viral hazards from bivalve molluscs, and other food matrices. In future steps, the magnetic bead-based method may further be improved by coating with anti-norovirus antibodies or porcine gastric mucin, which have a high affinity with HuNoV.

Compliance with Ethical Standards

Conflict of interest The authors declare that there are no conflicts of interest.

References

Atmar, R. L., Ramani, S., & Estes, M. K. (2018). Human noroviruses. *Current Opinion in Infectious Diseases, 31*(5), 422–432. https://doi.org/10.1097/QCO.0000000000000476.

Brié, A., Razafimahefa, R., Loutreul, J., Robert, A., Gantzer, C., Boudaud, N., & Bertrand, I. (2017). The Effect of Heat and Free Chlorine Treatments on the Surface Properties of Murine Norovirus. *Food and Environmental Virology, 9*(2), 149–158. https://doi.org/10.1007/s12560-016-9271-3.

Burkhardt, W., & Calci, K. R. (2000). Selective accumulation may account for shellfish-associated viral illness. *Applied and Environmental Microbiology, 66*(4), 1375–1378. https://doi.org/10.1128/AEM.66.4.1375-1378.2000.

Cannon, J. L., Papafragkou, E., Park, G. W., Osborne, J., Jaykus, L.-A., & Vinjé, J. (2006). Surrogates for the Study of Norovirus Stability and Inactivation in the Environment: A Comparison of Murine Norovirus and Feline Calicivirus. *Journal of Food Protection, 69*(11), 2761–2765. https://doi.org/10.4315/0362-028X-69.11.2761.

Chhabra, P., de Graaf, M., Parra, G. I., Chan, M. C. W., Green, K., Martella, V., et al. (2019). Updated classification of norovirus genogroups and genotypes. *The Journal of general virology, 100*(10), 1393–1406. https://doi.org/10.1099/jgv.0.001318.

Cook, N., Williams, L., & D'Agostino, M. (2019). Prevalence of Norovirus in produce sold at retail in the United Kingdom. *Food Microbiology, 79*, 85–89. https://doi.org/10.1016/J.FM.2018.12.003.

Costantini, V., Morantz, E. K., Browne, H., Ettayebi, K., Zeng, X.-L., Atmar, R. L., et al. (2018). Human Norovirus Replication in Human Intestinal Enteroids as Model to Evaluate Virus Inactivation. *Emerging Infectious Diseases, 24*(8), 1453–1464. https://doi.org/10.3201/eid2408.180126.

Coudray-Meunier, C., Fraisse, A., Martin-Latil, S., Guillier, L., & Perelle, S. (2013). Discrimination of infectious hepatitis A virus and rotavirus by combining dyes and surfactants with RT-qPCR. *BMC Microbiology, 13*(1), 216. https://doi.org/10.1186/1471-2180-13-216.

Cromeans, T., Park, G. W., Costantini, V., Lee, D., Wang, Q., Farkas, T., et al. (2014). Comprehensive comparison of cultivable norovirus surrogates in response to different inactivation and disinfection treatments. *Applied and Environmental Microbiology, 80*(18), 5743–5751. https://doi.org/10.1128/AEM.01532-14.

de Graaf, M., van Beek, J., & Koopmans, M. P. G. (2016). Human norovirus transmission and evolution in a changing world. *Nature Reviews Microbiology, 14*(7), 421–433. https://doi.org/10.1038/nrmicro.2016.48.

Ettayebi, K., Crawford, S., Murakami, K., Broughman, J., Karandikar, U., Tenge, V., et al. (2016). Replication of human noroviruses in stem cell–derived human enteroids. *Science, 353*(6306), 1387–1393. https://doi.org/10.1126/science.aaf5211.

Hatano, B., Kojima, A., Sata, T., & Katano, H. (2010). Virus detection using Viro-Adembeads, a rapid capture system for viruses, and plaque assay in intentionally virus-contaminated beverages. *Japanese journal of infectious diseases, 63*(1), 52–54.

Jones, M. K., Grau, K. R., Costantini, V., Kolawole, A. O., De Graaf, M., Freiden, P., et al. (2015). Human norovirus culture in B cells. *Nature Protocols, 10*(12), 1939–1947. https://doi.org/10.1038/nprot.2015.121.

Jones, M. K., Watanabe, M., Zhu, S., Graves, C. L., Keyes, L. R., Grau, K. R., et al. (2014). Enteric bacteria promote human and mouse norovirus infection of B cells. *Science, 346*(6210), 755–759. https://doi.org/10.1126/science.1257147.

Karim, M. R., Fout, G. S., Johnson, C. H., White, K. M., & Parshionikar, S. U. (2015). Propidium monoazide reverse transcriptase PCR and RT-qPCR for detecting infectious enterovirus and

norovirus. *Journal of Virological Methods, 219,* 51–61. https://doi.org/10.1016/J.JVIROMET.2015.02.020.

Kim, S. Y., & Ko, G. (2012). Using propidium monoazide to distinguish between viable and nonviable bacteria, MS2 and murine norovirus. *Letters in Applied Microbiology, 55*(3), 182–188. https://doi.org/10.1111/j.1472-765X.2012.03276.x.

Koo, H. L., Neill, F. H., Estes, M. K., Munoz, F. M., Cameron, A., DuPont, H. L., & Atmar, R. L. (2013). Noroviruses: The Most Common Pediatric Viral Enteric Pathogen at a Large University Hospital After Introduction of Rotavirus Vaccination. *Journal of the Pediatric Infectious Diseases Society, 2*(1), 57–60. https://doi.org/10.1093/jpids/pis070.

Langlet, J., Kaas, L., Croucher, D., & Hewitt, J. (2018). Effect of the Shellfish Proteinase K Digestion Method on Norovirus Capsid Integrity. *Food and Environmental Virology.* https://doi.org/10.1007/s12560-018-9336-6.

Le Guyader, F. S., Loisy, F., Atmar, R. L., Hutson, A. M., Estes, M. K., Ruvoën-Clouet, N., et al. (2006). Norwalk virus-specific binding to oyster digestive tissues. *Emerging Infectious Diseases, 12*(6), 931–936. https://doi.org/10.3201/eid1206.051519.

Lee, M., Seo, D. J., Seo, J., Oh, H., Jeon, S. B., Ha, S. D., et al. (2015). Detection of viable murine norovirus using the plaque assay and propidium-monoazide-combined real-time reverse transcription-polymerase chain reaction. *Journal of Virological Methods, 221,* 57–61. https://doi.org/10.1016/j.jviromet.2015.04.018.

Leifels, M., Jurzik, L., Wilhelm, M., & Hamza, I. A. (2015). Use of ethidium monoazide and propidium monoazide to determine viral infectivity upon inactivation by heat, UV- exposure and chlorine. *International Journal of Hygiene and Environmental Health, 218*(8), 686–693. https://doi.org/10.1016/J.IJHEH.2015.02.003.

Li, D., Baert, L., Xia, M., Zhong, W., Van Coillie, E., Jiang, X., & Uyttendaele, M. (2012). Evaluation of methods measuring the capsid integrity and/or functions of noroviruses by heat inactivation. *Journal of Virological Methods, 181*(1), 1–5. https://doi.org/10.1016/J.JVIROMET.2012.01.001.

Li, D., De Keuckelaere, A., & Uyttendaele, M. (2014). Application of long-range and binding reverse transcription-quantitative PCR to indicate the viral integrities of noroviruses. *Applied and Environmental Microbiology, 80*(20), 6473–6479. https://doi.org/10.1128/AEM.02092-14.

Manuel, C. S., Moore, M. D., & Jaykus, L.-A. (2018). Predicting human norovirus infectivity - Recent advances and continued challenges. *Food Microbiology, 76,* 337–345. https://doi.org/10.1016/J.FM.2018.06.015.

Martin, L. R., Duke, G. M., Osorio, J. E., Hall, D. J., & Palmenberg, A. C. (1996). Mutational analysis of the mengovirus poly(C) tract and surrounding heteropolymeric sequences. *Journal of virology, 70*(3), 2027–2031. https://doi.org/10.1128/jvi.70.3.2027-2031.1996.

Mathijs, E., Muylkens, B., Mauroy, A., Ziant, D., Delwiche, T., & Thiry, E. (2010). Experimental evidence of recombination in murine noroviruses. *Journal of General Virology, 91*(11), 2723–2733. https://doi.org/10.1099/vir.0.024109-0.

Mathijs, E., Stals, A., Baert, L., Botteldoorn, N., Denayer, S., Mauroy, A., et al. (2012). *A Review of Known and Hypothetical Transmission Routes for Noroviruses.* Food and Environmental Virology: Springer-Verlag. https://doi.org/10.1007/s12560-012-9091-z.

McLeod, C., Polo, D., Le Saux, J.-C., & Le Guyader, F. S. (2017). Depuration and Relaying: A Review on Potential Removal of Norovirus from Oysters. *Comprehensive Reviews in Food Science and Food Safety, 16*(4), 692–706. https://doi.org/10.1111/1541-4337.12271.

Moreno, L., Aznar, R., & Sánchez, G. (2015). Application of viability PCR to discriminate the infectivity of hepatitis A virus in food samples. *International Journal of Food Microbiology, 201,* 1–6. https://doi.org/10.1016/J.IJFOODMICRO.2015.02.012.

Nuanualsuwan, S., & Cliver, D. O. (2002). Pretreatment to avoid positive RT-PCR results with inactivated viruses. *Journal of Virological Methods, 104*(2), 217–225. https://doi.org/10.1016/S0166-0934(02)00089-7.

Patramool, S., Bernard, E., Hamel, R., Natthanej, L., Chazal, N., Surasombatpattana, P., et al. (2013). Isolation of infectious chikungunya virus and dengue virus using anionic polymer-coated magnetic beads. *Journal of Virological Methods, 193*(1), 55–61. https://doi.org/10.1016/J.JVIROMET.2013.04.016.

Payne, D. C., Vinjé, J., Szilagyi, P. G., Edwards, K. M., Staat, M. A., Weinberg, G. A., et al. (2013). Norovirus and medically attended gastroenteritis in US children. *The New England journal of medicine, 368*(12), 1121–1130. https://doi.org/10.1056/NEJMsa1206589.

Polo, D., Schaeffer, J., Teunis, P., Buchet, V., & Le Guyader, F. S. (2018). Infectivity and RNA persistence of a norovirus surrogate, the Tulane virus, in oysters. *Frontiers in Microbiology, 9,* 1–8. https://doi.org/10.3389/fmicb.2018.00716.

Randazzo, W., Khezri, M., Ollivier, J., Le Guyader, F. S., Rodríguez-Díaz, J., Aznar, R., & Sánchez, G. (2018). Optimization of PMAxx pretreatment to distinguish between human norovirus with intact and altered capsids in shellfish and sewage samples. *International Journal of Food Microbiology, 266,* 1–7. https://doi.org/10.1016/j.ijfoodmicro.2017.11.011.

Randazzo, W., López-Gálvez, F., Allende, A., Aznar, R., & Sánchez, G. (2016). Evaluation of viability PCR performance for assessing norovirus infectivity in fresh-cut vegetables and irrigation water. *International Journal of Food Microbiology, 229,* 1–6. https://doi.org/10.1016/j.ijfoodmicro.2016.04.010.

Randazzo, W., Piqueras, J., Rodríguez-Díaz, J., Aznar, R., & Sánchez, G. (2017). Improving efficiency of viability-qPCR for selective detection of infectious HAV in food and water samples. *Journal of Applied Microbiology, 124*(4), 958–964. https://doi.org/10.1111/jam.13519.

Rasff, T. R. A. S. for F. and F. (n.d.). No Title. https://webgate.ec.europa.eu/rasff-window/portal/?event=searchForm&cleanSearch=1. Accessed 15 April 2020

Razafimahefa, R., Ludwig-Begall, L., & Thiry, E. (2019). Cockles and mussels, alive, alive, oh - The role of bivalve molluscs as transmission vehicles for human norovirus infections. *Transboundary and Emerging Diseases.* https://doi.org/10.1111/tbed.13165.

Reed, L. J., & Muench, H. (1938). A simple method of estimating fifty per cent endpoints12. *American Journal of Epidemiology, 27*(3), 493–497. https://doi.org/10.1093/oxfordjournals.aje.a118408.

Rha, B., Lopman, B. A., Alcala, A. N., Riddle, M. S., & Porter, C. K. (2016). Incidence of Norovirus-Associated Medical Encounters among Active Duty United States Military Personnel and Their Dependents. *PLoS ONE, 11*(4), e0148505. https://doi.org/10.1371/journal.pone.0148505.

Richards, G. P. (2001). Enteric virus contamination of foods through industrial practices: A primer on intervention strategies. *Journal of Industrial Microbiology and Biotechnology, 27*(2), 117–125. https://doi.org/10.1038/sj.jim.7000095.

Sakudo, A., & Onodera, T. (2012). Virus capture using anionic polymer-coated magnetic beads (Review). *International Journal of Molecular Medicine.* https://doi.org/10.3892/ijmm.2012.962.

Sarmento, S. K., Guerra, C. R., Malta, F. C., Coutinho, R., Miagostovich, M. P., & Fumian, T. M. (2020). Human norovirus detection in bivalve shellfish in Brazil and evaluation of viral infectivity using PMA treatment. *Marine Pollution Bulletin, 157,* 111315. https://doi.org/10.1016/j.marpolbul.2020.111315.

Stals, A., Baert, L., Coillie, E. V., & Uyttendaele, M. (2012). Extraction of food-borne viruses from food samples : A review. *International Journal of Food Microbiology, 153*(1–2), 1–9. https://doi.org/10.1016/j.ijfoodmicro.2011.10.014.

Thackray, L. B., Wobus, C. E., Chachu, K. A., Liu, B., Alegre, E. R., Henderson, K. S., et al. (2007). Murine noroviruses comprising a single genogroup exhibit biological diversity despite limited sequence divergence. *Journal of virology, 81*(19), 10460–10473. https://doi.org/10.1128/JVI.00783-07.

Toldrà, A., Andree, K. B., Bertomeu, E., Roque, A., Carrasco, N., Gairín, I., et al. (2018). Rapid capture and detection of ostreid herpesvirus-1 from Pacific oyster Crassostrea gigas and seawater using magnetic beads. *PLoS ONE, 13*(10), e0205207. https://doi.org/10.1371/journal.pone.0205207.

Topping, J. R., Schnerr, H., Haines, J., Scott, M., Carter, M. J., Willcocks, M. M., et al. (2009). Temperature inactivation of Feline calicivirus vaccine strain FCV F-9 in comparison with human noroviruses using an RNA exposure assay and reverse transcribed quantitative real-time polymerase chain reaction—A novel method for predicting virus infectivity. *Journal of Virological Methods, 156*(1–2), 89–95. https://doi.org/10.1016/J.JVIROMET.2008.10.024.

Weinberg, G. A. (2018). Outbreak Epidemiology: One of Many New Frontiers of Norovirus Biology. *The Journal of Infectious Diseases*. https://doi.org/10.1093/infdis/jiy570.

Wigginton, K. R., & Kohn, T. (2012). Virus disinfection mechanisms: The role of virus composition, structure, and function. *Current Opinion in Virology, 2*(1), 84–89. https://doi.org/10.1016/j.coviro.2011.11.003.

Wigginton, K. R., Pecson, B. M., Sigstam, T., Bosshard, F., & Kohn, T. (2012). Virus inactivation mechanisms: Impact of disinfectants on virus function and structural integrity. *Environmental Science and Technology, 46*(21), 12069–12078. https://doi.org/10.1021/es3029473.

Wolf, S., Rivera-Aban, M., & Greening, G. E. (2009). Long-Range Reverse Transcription as a Useful Tool to Assess the Genomic Integrity of Norovirus. *Food and Environmental Virology, 1*(3–4), 129–136. https://doi.org/10.1007/s12560-009-9016-7.